



Full Text View

[Volume 28, Issue 12 \(December 1998\)](#)

Journal of Physical Oceanography

Article: pp. 2418–2426 | [Abstract](#) | [PDF \(183K\)](#)

The Coupling between Harbor Seiches at Palawan Island and Sulu Sea Internal Solitons*

Graham S. Giese, David C. Chapman, and Margaret Goud Collins

Woods Hole Oceanographic Institution, Woods Hole, Massachusetts

Rolu Encarnacion

Philippines Atmospheric, Geophysical and Astronomical Services Administration, Quezon City, Philippines

Gil Jacinto

Marine Science Institute, University of the Philippines, Quezon City, Philippines

(Manuscript received August 23, 1996, in final form February 4, 1998)

DOI: 10.1175/1520-0485(1998)028<2418:TCBHSA>2.0.CO;2

ABSTRACT

Between 1989 and 1991 the authors made observations that confirm and elucidate the coupling between harbor seiches at Puerto Princesa on Palawan Island in the Philippines and tide-generated internal solitons in the Sulu Sea. Published tidal current predictions for Basilan Strait in the Sulu Archipelago were used to produce an index to the daily ebb tidal flows near Pearl Bank where the solitons originate. The coherence between predicted maximum ebb tidal current speed and observed seiche activity was 0.60 and the phase lag between the two quantities closely matched published estimates of the time required for solitons to cross the Sulu Sea. Arrival of the Sulu Sea waves immediately offshore of Puerto Princesa in the form of internal bores corresponded in time to the initiation of harbor seiche activity. A more precise estimate of soliton travel time was determined from the time difference between predicted maximum ebb current and the initiation of seiche activity, and it was found to have a remarkably regular seasonal pattern, which can be largely explained by seasonal variations in Sulu Sea temperature and salinity stratification. Therefore, the timing of seiche events at Puerto Princesa can be forecast based on Sulu Archipelago tide predictions and soliton travel time. In general, the fortnightly pattern of seiche magnitude follows that of tidal current predictions, but day-to-day deviations are common. Seiche magnitude varies seasonally with generally low activity during the winter (northeast) monsoon and usually maximum activity late in the summer (southwest)

Table of Contents:

- [Introduction](#)
- [Puerto Princesa data](#)
- [Basilan Strait tidal](#)
- [Seasonal variation in](#)
- [Maximum amplitude seiches](#)
- [Discussion and summary](#)
- [REFERENCES](#)
- [FIGURES](#)

Options:

- [Create Reference](#)
- [Email this Article](#)
- [Add to MyArchive](#)
- [Search AMS Glossary](#)

Search CrossRef for:

- [Articles Citing This Article](#)


Search Google Scholar for:

- [Graham S. Giese](#)

- [David C. Chapman](#)
- [Margaret Goud Collins](#)
- [Rolu Encarnacion](#)
- [Gil Jacinto](#)

1. Introduction

Deep-sea surface waves provide significant amounts of energy to coastal processes at relatively short periods (1–100 s) by means of wind-generated surface waves, at short to intermediate periods (0.5–5 min) by means of infragravity waves, and at relatively long periods (12–24 h) by means of barotropic tides. However, the fundamental barotropic period of many coastal harbors, bays, and shelves lies within a range of 10–100 min and, except for tsunamis, oceanic surface wave spectra contain relatively little energy at those periods. Deep-sea internal wave spectra, in contrast, typically show an energy maximum within the period range 10–100 min, and in some cases a considerable amount of this energy is transported to coastal waters, sometimes generating a resonant response in the form of harbor seiches. These barotropic standing waves are commonly observed in the form of small amplitude, high frequency sea-level oscillations along exposed coasts, but occasionally, particularly in harbors, they can reach destructive proportions.


Puerto Princesa, the major port of Palawan Island in the Philippines ([Fig. 1](#) ) is especially well suited for the study of seiche excitation by tide-generated internal waves because of the unambiguous source of the large internal solitons that arrive there some 2½ days after they form in the vicinity of Pearl Bank in the Sulu Archipelago ([Apel et al. 1985](#)). Hazardous seiching at Puerto Princesa was described by [Haight \(1928\)](#) who attributed it to atmospheric forcing. More recently, [Giese and Hollander \(1987\)](#) used 60-year-old analog tide records to demonstrate that the seiches are related to semidiurnal tides at Puerto Princesa and, by inference, to the Sulu Sea tide-generated internal waves. Since that time, [Chapman and Giese \(1990\)](#) and [Grimshaw and Chapman \(1992\)](#) have elucidated the mechanism of energy transfer from internal waves to seiches, and [Giese et al. \(1990\)](#) have presented evidence of internal wave-produced seiche activity along the Caribbean coast of Puerto Rico.


In this report, we present new data gathered at Puerto Princesa between April 1989 and October 1991. The field observations include tide and temperature data recorded continuously within the harbor and CTD data recorded offshore during three short-term field studies. Using these data together with published tidal predictions from the Philippines National Mapping and Resource Information Authority (NAMRIA, 1989–91), we attempt to 1) correlate Puerto Princesa seiche activity with predicted tidal currents in the internal wave generation area, 2) explain the seasonal variations in seiche activity at Puerto Princesa, and 3) develop methodology for predicting seiche activity from tidal current predictions.

In [section 2](#) we describe and present examples of data obtained in the harbor and in offshore waters at Puerto Princesa, while in [section 3](#) we describe the relationship between Puerto Princesa seiche activity and the soliton-generating tidal currents at Pearl Bank. In [section 4](#) we illustrate and present the results of our calculation of the time required for solitons to transit the Sulu Sea, and we demonstrate that the observed seasonal variations in soliton travel time are primarily the result of seasonal variations in stratification of the Sulu Sea. [Section 5](#) contains an analysis of the variability in the occurrence of exceptionally vigorous harbor seiche activity, while [section 6](#) is devoted to a discussion and summary of the new results.

2. Puerto Princesa data

a. Harbor tide and temperature observations

An ENDECO Model 1152 tide, temperature, and salinity recorder was installed at the Puerto Princesa municipal pier ([Fig. 2](#) ) in April 1989. Measurements made at 5-min intervals were recorded on solid-state (EPROM) cartridges, which were replaced at approximately monthly intervals. Data cartridges were sent by mail to Woods Hole for downloading and data processing. The recorder remained in place and operated satisfactorily until its removal in November 1991. This recorder automatically compensates for changes in atmospheric pressure. It was not necessary to correct the data for changes in water density because of the shallow depth (approximately 3 m) of the pressure sensor and the relatively narrow range of temperature and salinity variations.

Large and well-defined sea-level oscillations with a period of about 75 min are a prominent feature of the tide records ([Fig. 3](#) ) local standard time at 120°E is used in this figure and throughout this report). Similar features have been described by [Haight \(1928\)](#) and [Giese and Hollander \(1987\)](#), who identified them as resonant oscillations of Puerto Princesa harbor. The geometry of the harbor and a calculation of its fundamental free mode of oscillation were presented in [Giese and Hollander \(1987\)](#). Briefly, the harbor's longitudinal axis has a length of approximately 13.6 km and a relatively constant seaward slope of about 0.005 from the head of the harbor to the shelf edge at a depth of approximately 70 m. Assuming a node at the shelf edge and an antinode at the harbor head, the fundamental free period was calculated to be about 70 min, ignoring friction. The municipal pier lies about one-third of the distance from the harbor head to the shelf edge. As would be expected, observations by [Haight \(1928\)](#) demonstrate that the height of seiches at the harbor head is larger than that recorded at the municipal pier.

The tidal influence on these oscillations is apparent from the semidiurnal, diurnal, and fortnightly modulations of their amplitude (Fig. 3). The typical fortnightly pattern has maximum activity about 5 days following syzygy (new or full moon) and smallest activity about 12 days following syzygy. Seiche activity also exhibits seasonal variability which is discussed in section 5.

The seawater temperature data also exhibit 75-min oscillations that typically have a phase opposite to that of the sea level oscillations, that is, maximum temperature tends to coincide with minimum sea level (Fig. 4a). The temperature and pressure sensors were only about 3 m deep, so it might be expected that near-surface temperature gradients in the harbor (Fig. 4b) would be responsible for the observed temperature oscillations at the municipal pier. However, boat traffic at the pier keeps the surface water fairly well mixed and our observations suggest that lateral variations in temperature are the primary cause of the temperature oscillations. Seaward-flowing warmer water from the upper harbor moves past the pier as sea level drops, and cooler water from the outer harbor flows past the pier as sea level rises. Such short term variations in surface water temperature are illustrated in Fig. 4c.

b. Offshore observations

In April 1989, when the Puerto Princesa tide recorder was established, we obtained vertical temperature profiles near the shelf edge offshore of the harbor (Fig. 2, station B) during the passage of several “rip bands” of choppy surface waves. The resulting data, which showed a sudden 2.5°C drop in near-bottom temperature, have been presented and discussed by Chapman et al. (1991). Although such rips are commonly associated with internal waves, the scale of these features was markedly smaller than the open water Sulu Sea rips described by Apel et al. (1985). It is suggested that the cold water represented one of a group of three or more near-bottom surges produced by the shoaling of a single deep-sea internal solitary wave, as in the laboratory experiments of Helfrich (1992).

Later, during March 1991, we attempted to record the signal produced by Sulu Sea internal solitary waves in deeper water. We had noticed that the tide record of 3 March (yearday 61) indicated a distinct change in seiche amplitude and cadence at about 1453 h (61.62 in yearday time), and we reasoned that similar changes might occur, somewhat later on subsequent days. We therefore established offshore station A (Fig. 2), where water depth was approximately 1000 m, in order to search for evidence of baroclinic processes coinciding in time with the anticipated seiche behavior changes. On each of the three following days, 4–6 March, we lowered a CTD to a depth of approximately 160 m, attached a small surface buoy to the line, and cast it free allowing the instrument to drift independently of the boat for periods varying between 3.75 and 4.35 h. The results (Figs. 5a–c, bottom curves) indicate that abrupt temperature increases of approximately 2°C occurred on each day (at about yeardays 62.67, 63.67, and 64.69). The temperature profile at station A (Fig. 5d) suggests that these changes were produced by vertical isotherm excursions of approximately 20 m.

The wind at station A was very light on 6 March (yearday 64) permitting observation of sea surface phenomena that often accompany large-amplitude internal waves. The sea surface became choppy with white caps at about 1630 h (yearday time 64.69; Fig. 5c) and stayed that way for about one-half hour and then gradually reverted to its previous condition. At about 1724 h (yearday time 64.72) surface slicks appeared at station A and remained in the area until we left it about an hour later.

Comparison of these results to the Puerto Princesa tide records for the same period (Figs. 5a–c, top curves) shows that the rapid 2°C temperature increases at station A coincided in time with abrupt variations in harbor seiche activity that were followed by oscillations with increased amplitude. We interpret this, in combination with previous observations, as evidence that these periods of enhanced seiche activity were produced by negative internal bores generated by the arrival of soliton packets.

3. Basilan Strait tidal currents and Puerto Princesa seiching

Apel et al. (1985) and Liu et al. (1985) describe the process by which strong ebb tidal flows across a narrow sill near Pearl Bank in the Sulu Archipelago produce baroclinic lee waves that cross the sill when the current turns and ultimately give rise to packets of rank-ordered internal solitons. The solitons propagate northwestward across the Sulu Sea, reaching the coast of Palawan Island in about 2½ days. Accordingly, with the objective of developing a predictive program for Puerto Princesa seiche activity, we sought to determine the relationship between daily seiche activity at Puerto Princesa and predicted tidal currents at the Sulu Archipelago.

The reference station for Sulu Archipelago tidal currents is at Basilan Strait, and prediction tables for this station are published annually by NAMRIA. According to the tables, the phase of tidal currents in the vicinity of Pearl Bank differs by only 5 minutes from those at Basilan Strait (e.g., NAMRIA 1991). Furthermore, Apel et al. (1985, their Fig. 5) found a direct relationship between predicted currents at Basilan Strait and both soliton amplitude and number in the Sulu Sea.

Therefore, we used predicted currents at Basilan Strait to produce the daily ebb tidal flows near Pearl Bank, I_{BS} , by calculating the sum of the squares of the daily predicted Basilan Strait ebb current maxima. Maximum predicted current speeds occasionally exceeded 3.5 m s^{-1} , while maximum values of I_{BS} sometimes exceeded $15 \text{ m}^2 \text{ s}^{-2}$. The square of current speed was used to produce an index that would be proportional to the energy of the soliton-producing maximum ebbs.

In order to produce an analogous time series of daily seiche activity at Puerto Princesa, we first performed a harmonic analysis of the sea-level data, predicted the astronomical tide, and subtracted it from the original time series. We then calculated the daily sea-level variance of the residual record for the frequency band between 13.0 and 27.4 cpd (0.009–0.019 cpm), which dominated the record (e.g., see [Fig. 7](#)). The units of the variance time series are $\text{m}^2 \text{ cpm}^{-1}$, making it comparable to I_{BS} . The two time series are shown together in [Fig. 6a](#).

The coherence and phase relationships between the two time series are presented in [Figs. 6b and 6c](#). The coherence at 14.5 days (0.069 cpd; close to the tidal fortnightly period) is 0.60. The phase delay at 0.069 cpd is 2.22 days with I_{BS} leading the seiche activity. Reducing this by 0.13 days to account for the expected time delay between maximum ebb current and slack water produces an estimated phase lag of 2.09 days. These results demonstrate that Basilan Strait tidal predictions can serve as a useful predictor of Puerto Princesa seiche activity.

4. Seasonal variation in soliton travel time

a. Results from seiche observation and tide prediction

At times the residual sea-level record from Puerto Princesa exhibits “bursting,” a sudden increase in activity that both abruptly terminates and far exceeds the previously existing background seiching. The time of initiation of bursting can be determined by visual analysis of the sea-level data ([Fig. 7](#)). Assuming that seiche activity is initiated by the arrival of Sulu Sea internal soliton packets following the model proposed by [Chapman and Giese \(1990\)](#), and assuming that the solitons cross the Sulu Sea in approximately 2.5 days, a more precise estimate of travel time for specific days can be calculated making use of the measured time of seiche burst initiation and the predicted time of maximum ebb current at Pearl Bank approximately 2.5 days earlier. In calculating soliton travel time, we assumed the delay between maximum ebb current and departure of the “wave” from Pearl Bank to be 3.1 h, based on the observations reported in [Apel et al. \(1985\)](#) that the tide-produced baroclinic disturbances cross the bank at about the time of slack water.

To provide an example of this calculation, an asterisk has been placed on [Fig. 7](#) to designate the time that seiche bursting began on 15 October 1990, at approximately yearday 287.818 ± 0.002 . Seeking a Pearl Bank ebb current maximum approximately 2.5 days earlier in the table of current predictions, we find an ebb maximum on 13 October at 0844 h or yearday 285.364, which yields a time delay between the two of 2.454 days (58.9 h) and a soliton travel time of 2.325 days (55.8 h). This travel time corresponds to a phase speed of 2.24 m s^{-1} , assuming the distance between Pearl Bank and Puerto Princesa to be 450 km.

Similar calculations of soliton travel time were carried out for 103 occasions on which the initiation of seiche bursting at Puerto Princesa was particularly distinct and the results are presented in [Fig. 8](#) (solid curves). The mean value of all data points, 55.8 h, is indicated by dotted horizontal lines. The mean phase speed of Sulu Sea solitons is 2.24 m s^{-1} and the range extends from 1.99 to 2.61 m s^{-1} . [Apel et al. \(1985\)](#) found the range of phase speeds for deep water internal solitons in the middle of the Sulu Sea in May 1980 to be 1.8– 2.6 m s^{-1} .

b. Results from historical hydrographic data

To account for the observed seasonal variations in [Fig. 8](#), we have calculated seasonal variations in the time required for internal waves to cross the Sulu Sea based on historical hydrographic data. We obtained temperature and salinity profiles ([NOAA/NODC 1991](#)) for the area outlined in [Fig. 1](#), grouped them by month, and estimated single vertical profiles to represent each month. Below a depth of 300 m no seasonal variations were apparent and the same temperature and salinity distributions were used for all months. Because no salinity observations within the study area were available for the months of February and November, the analysis was carried out for only 10 months.

Next, we calculated the vertical density gradient for each month ([Millero et al. 1980](#); [Millero and Poisson 1981](#)) and used those profiles to calculate the corresponding mode-one internal wave phase speeds (e.g., [Gill 1982](#)) and the times required to travel 450 km. The results are displayed in [Fig. 8](#) by dashed lines. The mean phase speed of Sulu Sea internal waves was found by this method to be 2.26 m s^{-1} and the mean time to travel 450 km to be 55.3 h.

The similarity of the two curves shown on [Fig. 8](#) shows that the observed seasonal variations in soliton travel time can be explained to a large degree by the seasonal variations in stratification in the Sulu Sea. Furthermore, despite the obvious limitations of these estimates, [Fig. 8](#) indicates that the initiation of seiche bursting at Puerto Princesa is a reliable indicator of Sulu Sea soliton arrival time. We have not explored the possible implications of the anomalies in seasonal travel time indicated in [Fig. 8](#). We suggest, however, that future researchers with access to more extensive data may wish to investigate both seasonal and long-term soliton travel time variations as indicators of meteorological and climatic variability.

5. Maximum amplitude seiches

Daily Puerto Princesa sea-level variance at the fundamental seiche frequency (0.009–0.019 cpm), based on all tide data obtained during this study, is presented in [Fig. 9](#). The variance analysis was performed on the residual sea-level data after removal of the astronomical tides as described in [section 3](#) above. The time of perigean and near-perigean new or full moon and the difference (in days) between the times of perigee and new or full moon ($|P - S|$) are indicated on the figure. The prevailing wind conditions for the Sulu Sea—northeast monsoons, southwest monsoons, and transitional periods—are also indicated.

Comparing [Figs. 8](#) and [9](#) we note that the annual variation of soliton travel time is more strikingly evident than the annual variation of seiche activity. For example, [Fig. 9](#) indicates a tendency for seiche activity to increase during the semiannual relatively calm transitions between the two monsoon periods. Turbulence due to wind stress during the windy monsoons would be expected to contribute to soliton dissipation, thus increased seiche activity during the transitional periods may result from decreased wind-produced soliton dissipation.

Nevertheless, a correspondence is evident between vigorous seiche activity at Puerto Princesa and low soliton travel time during summer, typically between yeardays 200 and 300. Such a correspondence might be expected based on the work of [Liu et al. \(1985\)](#), who showed that fully developed soliton packets lose amplitude through turbulent dissipation (as well as radial spreading). One would expect faster summer solitons to experience less dissipation and therefore to reach Puerto Princesa with relatively more energy than initially similar winter solitons.

We have explored this relationship using only data from 1990 and 1991, when both winter and summer data are available, and we focus attention on the fortnightly occurring periods of maximum seiche activity. From [Fig. 9](#), we estimate a value of $0.6 \text{ m}^2 \text{ cpm}^{-1}$ to represent very large summer activity and $0.2 \text{ m}^2 \text{ cpm}^{-1}$ to represent very large winter activity. Taking the square roots of these values to derive quantities proportional to wave amplitude, we estimate a summer-to-winter seiche activity ratio of 1.7.

This can be compared to the analogous ratio of internal soliton amplitude in summer at Palawan Island to that in winter based on the results of [Liu et al. \(1985\)](#). Again only data from 1990 and 1991 are used for this calculation. From [Fig. 8](#), a representative summer travel time is 54 h, while a representative winter travel time is 60 h. Referring to [Fig. 7](#) from [Liu et al. \(1985\)](#) and taking 6 h as the travel time difference, the summer-to-winter soliton amplitude ratio is approximately 1.1.

Thus, we find that decreased energy dissipation due to decreased soliton travel time can account for some (about 10%) increase in Puerto Princesa seiche activity during summer, but it alone cannot account for the observed differences between seasonal maximum and minimum activity (about 70%). It seems likely that wind-produced turbulence and circulation contribute significantly to the observed seasonal differences, especially since increased travel time increases soliton susceptibility to these processes and since the strongest winds are associated with the winter monsoon. As further illustration of the likely role of wind-produced dissipation, we note that during each of the three calendar years for which we have data, there are month-long periods during summer when both soliton travel time and Puerto Princesa seiche activity are small. Particularly impressive in this respect is the period of small seiche activity following the perigean new moon of 12 July 1991 (yearday 192 on bottom panel of [Fig. 9](#)) despite strong predicted tidal currents and small soliton travel times. Furthermore, if the swath of radial spreading shifts southward during the winter monsoon (see [Fig. 1](#)), then Puerto Princesa would probably receive smaller solitons.

6. Discussion and summary

a. Timing of Puerto Princesa seiching events

The results of this study confirm that harbor seiches at Puerto Princesa, first described by [Haight \(1928\)](#), are forced by remotely generated Sulu Sea internal solitons. Because the Sulu Sea solitons are tide generated ([Apel et al. 1985](#)), the initiation of harbor seiching events can be forecast using existing tidal current predictions together with estimates of seasonal variations in soliton travel time. Based on the combination of a 30-month tide record from Puerto Princesa and published current predictions for Basilan Strait, we find that seasonal variations in soliton travel time are remarkably regular. Maximum and minimum travel times are about 10% above and below the mean value and occur toward the ends of the northeast

(winter) and southwest (summer) monsoon periods, respectively.

From both observation and modeling results, [Apel et al. \(1985\)](#) have described the nonlinear effect of soliton amplitude on travel time. That relationship can also be inferred from the Puerto Princesa seiche activity data presented in [Fig. 9](#). During late summer, fortnightly variations between maximum and minimum daily activity sometimes exceed an order of magnitude, while corresponding variations in the forcing tidal currents as indicated by the index I_{BS} are approximately half that value. Part of the difference can probably be explained by the decrease in both travel time and dissipation of the larger amplitude solitons generated by spring tides.

Nevertheless, the similarity between travel time calculated from Puerto Princesa seiche events and calculated from Sulu Sea historical hydrographic conditions ([Fig. 8](#)) demonstrates that the seasonal variation in soliton travel time observed in this study was primarily produced by seasonal variations in Sulu Sea density stratification rather than a similar seasonal variation in soliton amplitude. Not only does this result strengthen confidence in prediction of the timing of seiche events, but it suggests the possibility of using variations in soliton travel time as determined from seiche data and tide predictions as an indicator of variations in Sulu Sea hydrographic conditions and, over extended time periods, global climatic conditions.

b. Magnitude of Puerto Princesa seiching events

While fortnightly tidal current variation at the Sulu Archipeligo is a useful predictor for episodes of maximum seiche activity, it does not predict the magnitude of those episodes. In addition, large day-to-day variations in seiche magnitude are common within a fortnightly cycle. Also, while seasonal variations in seiche magnitude are apparent, those variations are not steady. The most consistent characteristics are the occurrence of extreme seiche activity toward the end of the southwest monsoon and the lack of extreme activity during the northeast monsoon.

Turbulence produced by wind stress acting at the surface of the Sulu Sea probably plays an important role in determining soliton amplitude and, therefore, seiche magnitude, at all timescales, and soliton dissipation as a function of travel time is a significant factor in determining seasonal variations of seiche magnitude. It is also likely that a significant role is played by factors in the soliton generation area, other than tidal current speed, that affect initial internal wave magnitudes—specifically, local winds, subtidal-frequency currents and water density stratification. Modeling studies are presently underway to explore the effects of such factors on internal wave, and seiche, characteristics.

Acknowledgments

We are grateful to Ernani Menez, Director of the Smithsonian Sorting Center, for his assistance in planning field studies; to Wernito Amores Masangcap of the Philippine Atmospheric, Geophysical and Astronomical Services Administration, and Norman Songco of Puerto Princesa for assistance with instrument deployment and maintenance; and to Benjamin Giese of Texas A&M University, and George Heimerdinger of the National Oceanographic Data Center for providing historical data; and to an anonymous referee for providing helpful comments. Major funding was provided by the National Science Foundation under Grant INT-8816481 from the International Division, East Asia Regional Program and under Grant OCE-8923065 from the Ocean Sciences Division; and by the Office of Naval Research under Grant N00014-92-J-1200. Additional support was provided by an Independent Study Award from the Woods Hole Oceanographic Institution, by the Institution's Coastal Research Center and by the Institution's Sea Grant Program under NOAA Grant NA46RG0470.

REFERENCES

Apel, J. R., J. R. Holbrook, A. K. Liu, and J. J. Tsai, 1985: The Sulu Sea internal soliton experiment. *J. Phys. Oceanogr.*, **15**, 1625–1651..

Chapman, D. C., and G. S. Giese, 1990: A model for the generation of coastal seiches by deep-sea internal waves. *J. Phys. Oceanogr.*, **20**, 1459–1467..

—, M. G. Collins, R. Encarnacion, and G. Jacinto, 1991: Evidence of internal swash associated with Sulu Sea solitary waves? *Contin. Shelf Res.*, **11**, 591–599..

Giese, G. S., and R. B. Hollander, 1987: The relationship between coastal seiches at Palawan Island and tide-generated internal solitary waves in the Sulu Sea. *J. Geophys. Res.*, **92**, 5151–5156..

—, D. C. Chapman, P. G. Black, and J. A. Fornshell, 1990: Causation of large-amplitude coastal seiches on the Caribbean coast of Puerto Rico. *J. Phys. Oceanogr.*, **20**, 1449–1458..

Gill, A. E., 1982: *Atmosphere–Ocean Dynamics*. Academic Press, 662 pp..

Grimshaw, R. H. J., and D. C. Chapman, 1992: Continental shelf response to forcing by deep-sea internal waves. *Dyn. Atmos. Oceans*, **16**, 355–378..

Haight, F. J., 1928: Unusual tidal movements in the Sulu Sea. *Military Eng.*, **20**, 471–475..

Helfrich, K. R., 1992: Internal solitary wave breaking and run-up on a uniform slope. *J. Fluid Mech.*, **243**, 133–154..

Liu, A. K., J. R. Holbrook, and J. R. Apel, 1985: Nonlinear internal wave evolution in the Sulu Sea. *J. Phys. Oceanogr.*, **15**, 1613–1624..

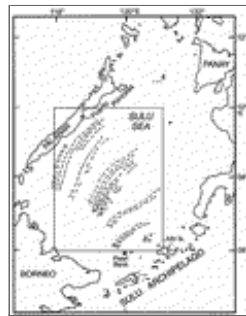
Millero, F. J., and A. Poisson, 1981: International one-atmosphere equations of state of seawater. *Deep-Sea Res.*, **28**, 625–629..

—, C.-T. Chen, A. Bradshaw, and K. Schleicher, 1980: A new high pressure equation of state for seawater. *Deep-Sea Res.*, **27**, 255–264..

NAMRIA, 1991: *Predicted Tide and Current Tables*. National Mapping and Resource Information Authority, Fort Bonifacio, Makati, Metro Manila, 229 pp..

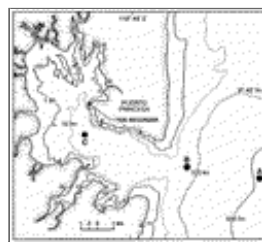
NOAA/NODC, 1991: *Global Ocean Temperature and Salinity Profiles*. CD-ROM NODC-03. National Oceanographic Data Center, Washington, DC..

Figures



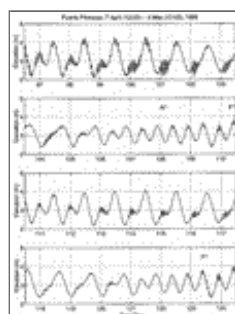
Click on thumbnail for full-sized image.

Fig. 1. Location of Palawan Island, the Sulu Sea, and the Sulu Archipeligo in the Philippines. Dashed lines represent the surface expression of internal solitons that are generated by strong tides near Pearl Bank and that travel northwestward, reaching Puerto Princesa in about 2.5 days (after [Apel et al. 1985](#)).



Click on thumbnail for full-sized image.

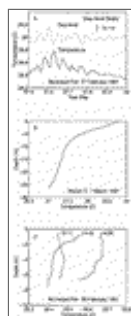
Fig. 2. Puerto Princesa and offshore waters showing location of the tide recorder and stations **A** (deep water), **B** (shelf edge), and **C** (inner harbor).



Click on thumbnail for full-sized image.

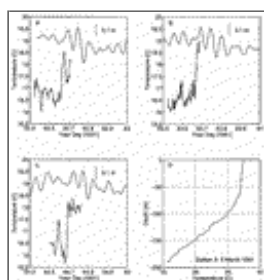
Fig. 3. The first 28 days of tidal data from Puerto Princesa illustrating the semidiurnal, diurnal, and fortnightly modulation of

seiche activity. Times of lunar apogee (*A*), lunar perigee (*P*), and full moon (*F*) are labeled. In addition to events shown, new moon and perigee occurred on 6 April (yearday 95) and new moon on 5 May (yearday 124). Note that the largest seiche oscillations have a larger amplitude than the smallest semidiurnal tides.



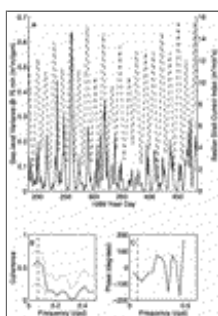
[Click on thumbnail for full-sized image.](#)

Fig. 4. (a) Water temperature at Puerto Princesa tide station for a 12-h period (solid line) compared with sea-level data for the same period (dotted line). (b) Water temperature profile at station C in Puerto Princesa harbor at 1415 h local time. (c) Three temperature profiles from the tide station taken over a 29-minute period during seiching. Note the different depth scales in (b) and (c).



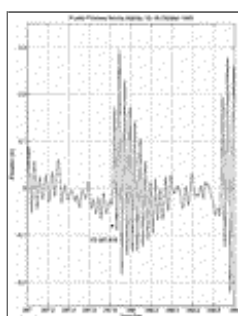
[Click on thumbnail for full-sized image.](#)

Fig. 5. (a)–(c). The bottom curve of each panel shows water temperature for periods of about 4 h at a depth of about 160 m at station A. The upper curve shows portions of the Puerto Princesa tide record (with astronomical tides removed) for corresponding, but longer, time periods. (d) Typical temperature profile at station A during the experiment.



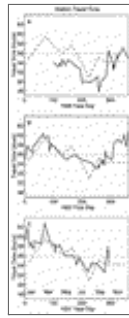
[Click on thumbnail for full-sized image.](#)

Fig. 6. The relationship between predicted maximum ebb currents at Basilan Strait and observed seiche activity at Puerto Princesa. (a) Index of predicted daily maximum ebb tidal current at Basilan Strait (I_{BS} ; dashed curve) and observed daily seiche activity at Puerto Princesa (solid curve). Note that greatest seiche activity generally occurs several days after maximum tidal currents. (b) Coherence and (c) phase between the two time series in (a) with 20 degrees of freedom. The dotted curves in (b) show the 90% confidence limits. The dashed vertical line denotes a frequency of 0.069 cpd (14.5 days).



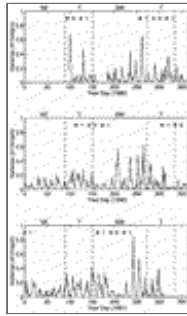
[Click on thumbnail for full-sized image.](#)

Fig. 7. Residual sea level (after removal of astronomical tides) at Puerto Princesa for 15 and 16 October 1990, illustrating the abrupt initiation of harbor seiche bursting that sometimes occurs there. The asterisk designates the beginning of a period of vigorous seiching at yearday 287.818. Another such period begins a little more than 24 h later.



[Click on thumbnail for full-sized image.](#)

Fig. 8. (a)–(c). Computed internal soliton travel time between Pearl Bank and Puerto Princesa for the study period (solid curves). The mean travel time, 55.8 h, is indicated by horizontal dotted lines. The dashed lines indicate the mean monthly travel time of mode one internal waves calculated from historical temperature and salinity profiles.



[Click on thumbnail for full-sized image.](#)

Fig. 9. Daily Puerto Princesa sea-level variance ($\text{m}^2 \text{cpm}^{-1}$) at seiche frequency (0.009–0.019 cpm) for the study period. Asterisks denote new or full moon in close association with perigee. The associated numerals give the difference (in days) between the two. Vertical dashed lines separate periods of northeast monsoons (NE) and southwest monsoons (SW) from transitional periods (T).

* Woods Hole Oceanographic Institution Contribution Number 9343.

Corresponding author address: Dr. Graham S. Giese, Woods Hole Oceanographic Institution, Woods Hole, MA 02543.

E-mail: ggiese@whoi.edu

[top ▲](#)



© 2008 American Meteorological Society [Privacy Policy and Disclaimer](#)
Headquarters: 45 Beacon Street Boston, MA 02108-3693
DC Office: 1120 G Street, NW, Suite 800 Washington DC, 20005-3826
amsinfo@ametsoc.org Phone: 617-227-2425 Fax: 617-742-8718
[Allen Press, Inc.](#) assists in the online publication of AMS journals.